Transport in Porous Media **49:** 9–25, 2002.

Convective Plume Paths in Anisotropic Porous Media

D.A.S. REES[1], L. STORESLETTEN[1,2] and ANDREW P. BASSOM[3]
[1]*Department of Mechanical Engineering, University of Bath, Claverton Down, Bath, BA2 7AY, U.K.*
[2]*Department of Mathematics, Agder University College, Serviceboks 422, 4604 Kristiansand, Norway*
[3]*School of Mathematical Sciences, University of Exeter, North Park Road, Exeter, EX4 4QE, U.K.*

(Received: 27 October 2000)

Abstract. Free convection motions induced by point sources or horizontal line sources of heat are usually assumed to take the form of a vertically orientated plume. In this paper we consider how material anisotropy affects the path of the plume centreline and we show that it is strongly affected by both the anisotropy and the presence of impermeable bounding surfaces. The plume path is a straight line whose angle from the vertical is determined by a balance between the upward buoyancy force, the need for the plume to entrain equal amounts of fluid from the external regions either side of it, and the ease of fluid motion in the direction of the principal axis with the highest permeability.

Key words: free convection, line heat source, anisotropy, plume path.

Nomenclature

a_0, b_0	scalings for the leading order boundary layer solution.
a_1, b_1	scalings for the first order boundary layer solution.
A, B, $\hat{B}$, C, D	coefficient functions.
$\overline{A}$, $\overline{B}$, $\overline{C}$	coefficient functions.
C_p	specific heat.
d	length scale.
f_0, g_0	leading terms in the boundary layer expansion.
f_1, g_1	first order terms in the boundary layer expansion.
F_0, G_0	scaled leading order terms in the boundary layer expansion.
F_1, G_1	scaled first order terms in the boundary layer-expansion.
$\mathcal{F}$	leading order outer region solution.
g	gravity.
$(\underline{i}, \underline{j}, \underline{k})$	unit vectors in the directions of the principal axes.
K	permeability.
$\underline{\underline{K}}$	permeability tensor.
L	scaled permeability.
M_1, M_2, M_3	constants of integration.
q'	rate of heat flux per unit length of the line source.
r	radial coordinate.

R	Darcy–Rayleigh number.
X, Y	x and y coordinates after rotation through an angle δ.

Greek Letters

α, β, γ	rotation angle of the principal axes about the x-, y- and z-axes.
$\hat{\beta}$	coefficient of thermal expansion.
δ	direction of the plume centreline.
ζ	scaled similarity variable.
η	similarity variable.
θ	temperature.
κ	thermal diffusivity.
μ	viscosity.
ξ	permeability ratio.
ρ	density.
ϕ	angular coordinate relative to the upward vertical.
ϕ^+, ϕ^-	angular positions of the bounding surfaces.
Φ	angular coordinate relative to $\phi = \delta$.
ψ	streamfunction.

Superscripts and subscripts

1, 2, 3	denotes the three principal axes.
*	dimensional.
∞	ambient.
x, y	derivatives with respect to x and y, respectively.
X, Y	derivatives with respect to X and Y, respectively.
$'$	derivatives with respect to either η or ζ.
$+$	region for which $\phi > \delta$.
$-$	region for which $\phi < \delta$.

1. Introduction

It is a matter of common experience that atmospheric plumes rise vertically in otherwise still air, but that their path may deviate quite substantially from this in the presence of wind. Such deviations were also found by Shaw (1985) for plume flow in a confined region with distinct inlets and outlets of fluid. Other effects, such as entrainment into a bounding surface and the merging of neighbouring plumes, both of which yield curved plume paths, have been summarised in the review paper of Gebhart (1979). Below groundlevel the presence of groundwater flow (together with other effects such as heterogeneities and variable saturation) also serves to modify the path taken by a contaminant plume in a porous medium; see Harter and Yeh (1996a, b) for example. However, when forced convective effects are absent, the resulting free convective plume is usually assumed to ascend vertically.

In our previous paper (Bassom *et al.*, 2001) we considered a very much simpler configuration than those of Harter and Yeh by restricting attention to a horizontal line heat source embedded in a fully saturated isotropic porous medium. Although such a situation had already been studied previously by Afzal (1985), we extended his analysis to cases where the porous medium is bounded by two semi-infinite surfaces at arbitrary angles. It was found that the free convective plume alway deviates

from its vertical path unless the bounding surfaces are symmetrically placed with respect to the vertical. Further, the paper by Bassom *et al.* (2001) gives a simple analytical expression relating the plume deviation and the angles of the bounding surfaces. The reason for such deviations lies in the competing effects of buoyancy, which causes an upwards force, and the need for the plume to entrain roughly the same amount the fluid from the external regions lying on each side of the plume.

However, many naturally occuring porous media are anisotropic with respect to their material properties. Few studies have examined how boundary layers react to the presence of anisotropy. To our knowledge only three exist to date: Ene (1991), Rees and Storesletten (1995) and Storesletten and Rees (1997). In these studies the boundary layer always remains attached to the heated surface, but for a free convective plume there is no surface to guide its upward path. In the light of the results of Bassom *et al*. (2001) it seems likely that anisotropy might have the same qualitative effect as the presence of an asymmetric bounding surface in an isotropic medium because of the breaking of symmetries. Therefore the aim of the present paper is to determine the effects of anisotropy on the angle which the plume centreline makes with the vertical. We consider three different configurations: an isolated line source, a line source placed at the end of a semi-infinite surface (which serves to restrict the flow in the region outside the plume) and a line source embedded in a plane surface.

To begin we suppose that the line source is placed at the intersection of two bounding planes, more details of which are given below, and we concentrate on the behaviour of the plume at large distances from the source. Depending on the configuration studied, the flow is divided into various regions, one of which is the boundary layer (i.e. the plume or inner) region, and either one (in the case of an isolated line source) or two outer regions (when the porous region forms a wedge with the plume at the apex). The last of these three cases is illustrated in Figure 1.

2. Mathematical Formulation

The present work deals with natural convective flow arising from a horizontal line source of heat embedded in a porous medium with anisotropic permeability. A Cartesian frame of reference is chosen where the x-axis is in the upward vertical direction and the y- and z-axes are both horizontal and aligned normal to and along the line source, respectively. The permeability tensor, $\underline{\underline{K}}$, is given by

$$\underline{\underline{K}} = K_1 \underline{i}'\underline{i}' + K_2 \underline{j}'\underline{j}' + K_3 \underline{k}'\underline{k}', \tag{1}$$

where the right-handed set of unit vectors, $\underline{i}'$, $\underline{j}'$ and $\underline{k}'$ are obtained by rotating the unit vectors in the x-, y- and z-directions (respectively, $\underline{i}$, $\underline{j}$ and $\underline{k}$) by an angle α about the x-axis, followed by a rotation of an angle β about the y-axis and an angle γ about the z-axis, in that order. In other words we have

$$\underline{i}' = (\cos\beta\cos\gamma, \cos\beta\sin\gamma, -\sin\beta) \tag{2a}$$

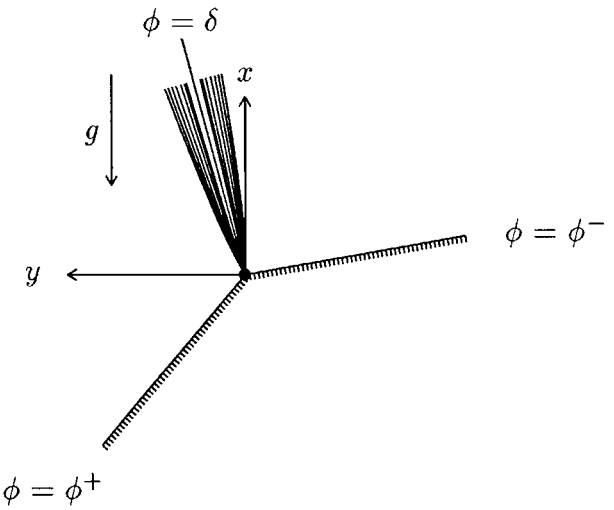

Figure 1. Schematic diagram of the flow configuration depicting two bounding surfaces at $\phi = \phi^+$ and $\phi = \phi^-$, and the plume with centreline along $\phi = \delta$. Also shown are the x- and y- axes ($\phi = 0$ and $\phi = 90°$, respectively) and the direction of gravity. We also consider cases with only one bounding surface and with no bounding surfaces.

$$\underline{j}' = (-\cos\alpha \sin\gamma + \sin\alpha \sin\beta \cos\gamma, \cos\alpha \cos\gamma + \\ + \sin\alpha \sin\beta \sin\gamma, \sin\alpha \cos\beta) \tag{2b}$$

$$\underline{k}' = (\sin\alpha \sin\gamma + \cos\alpha \sin\beta \cos\gamma, -\sin\alpha \cos\gamma + \\ + \cos\alpha \sin\beta \sin\gamma, \cos\alpha \cos\beta). \tag{2c}$$

The permeability matrix can now be written in the symmetric form,

$$\underline{\underline{K}} = K_1 \begin{pmatrix} L_{11} & L_{12} & L_{13} \\ L_{12} & L_{22} & L_{23} \\ L_{13} & L_{23} & L_{33} \end{pmatrix}, \tag{3}$$

where K_1 is used as the reference permeability, and the L_{ij} values are given in the Appendix.

We consider steady flow in a porous medium for which Darcy's law and the Boussinesq approximation are both valid. Although the medium is anisotropic and hence fluid motion will, in general, be induced in the z-direction, there is no resulting z-variation in the convecting plume. Therefore, the governing equations are reduced to

$$L_{11}\psi_{xx} + 2L_{12}\psi_{xy} + L_{22}\psi_{yy} = (L_{11}L_{22} - L_{12}^2)\theta_y, \tag{4a}$$

$$\theta_{xx} + \theta_{yy} = \psi_y\theta_x - \psi_x\theta_y, \tag{4b}$$

$$w = \frac{(L_{13}L_{22} - L_{12}L_{23})\psi_y + (L_{12}L_{13} - L_{11}L_{23})\psi_x}{(L_{11}L_{22} - L_{12}^2)} \tag{4c}$$

where

$$u = \frac{\partial \psi}{\partial y}, \qquad v = -\frac{\partial \psi}{\partial x} \tag{5}$$

and w are the seepage velocities in the x-, y- and z-directions, respectively. Here ψ is the streamfunction and θ is the temperature. All the variables in (4) have been made dimensionless using the transformations

$$\psi^* = \kappa\psi, \qquad (x^*, y^*, z^*) = \frac{C_p\mu\kappa^2}{g\hat{\beta}K_1q'}(x, y, z), \qquad \theta^* = \theta_\infty + \frac{q'}{\rho C_p\kappa}\theta, \tag{6}$$

where starred terms denote dimensional/unscaled quantities, q' represents the rate of heat flux per unit length of the line source, and other terms, which have their usual meanings in the porous medium context, are given in the Nomenclature. We note that there is no Darcy–Rayleigh number present in Equations (4); if we define

$$d = \frac{C_p\mu\kappa^2}{g\hat{\beta}K_1q'}, \tag{7}$$

as a natural lengthscale, then the Darcy–Rayleigh number, which for a line source is defined as

$$R = \frac{\rho g\hat{\beta}K_1d}{\mu\kappa}\left(\frac{q'}{\rho C_p\kappa}\right), \tag{8}$$

is equal to unity.

We will be considering the boundary layer flow induced by a line source and therefore the width of the plume is asymptotically small compared with the distance from the leading edge. Far away from the plume centreline the velocity and temperature approach their respective ambient values:

$$\psi_y \to 0, \qquad \theta \to 0 \quad \text{as} \quad y \to \infty. \tag{9}$$

This condition will need to be made more precise below when we consider the detailed effect of the isothermal flow induced in the regions either side of the plume. The dimensionless heat flux per unit length released by the horizontal line source is now unity. The equation for the global conservation of heat takes the form,

$$\int_{-\infty}^{\infty} (\psi_y\theta - \theta_x)\, dy = 1, \tag{10}$$

where it is noted that the infinite limits represent the mathematical problem from the point of view of the plume boundary layer.

3. Analysis

The analysis we reproduce below is very closely related to that given in Bassom *et al*. (2001) and it uses the method of matched asymptotic expansions. The plume is assumed to have its centreline laying at an unknown angle δ to the vertical and the basic boundary layer flow is determined. Entrainment into the plume induces a flow in the outer region or regions which must be computed numerically, unlike the isotropic problem considered in Bassom *et al.* (2001) where a simple analytical solution exists. In turn, the outer flow causes a small correction to the plume solution, but the equations governing this leading correction to the plume have a solution only when δ takes the correct value.

3.1. THE INNER REGION

We begin by rotating the coordinate axes through the angle, δ, which is currently unknown. Relative to polar coordinates (r, ϕ) the positive x-axis corresponds to $\phi = 0$, the y-axis to $\phi = \pi/2$, and the bounding surfaces to $\phi = \phi^+$ and $\phi = \phi^-$, as shown in Figure 1. The new coordinates, X and Y, obtained by rotation, are given by

$$X = x\cos\delta + y\sin\delta, \qquad Y = -x\sin\delta + y\cos\delta. \tag{11a, b}$$

The transformed governing equations are then

$$A\psi_{XX} + 2B\psi_{XY} + C\psi_{YY} = D\tan\delta\theta_X + D\theta_Y, \tag{12a}$$

$$\theta_{XX} + \theta_{YY} = \psi_Y\theta_X - \psi_X\theta_Y, \tag{12b}$$

and the energy constraint becomes

$$\int_{-\infty}^{\infty} [\psi_X\theta\sin\delta + \psi_Y\theta\cos\delta - \theta_X\cos\delta + \theta_Y\sin\delta]\, dY = \cos\delta, \tag{13}$$

where the new coefficients in (12a) are defined as

$$A = L_{11}\cos^2\delta + L_{12}\sin 2\delta + L_{22}\sin^2\delta, \tag{14a}$$

$$B = \frac{1}{2}(L_{22} - L_{11})\sin 2\delta + L_{12}\cos 2\delta, \tag{14b}$$

$$C = L_{11}\sin^2\delta - L_{12}\sin 2\delta + L_{22}\cos^2\delta, \tag{14c}$$

$$D = (L_{11}L_{22} - L_{12}^2)\cos\delta. \tag{14d}$$

The boundary layer solution takes the following form as $X \to \infty$:

$$\psi = X^{1/3} f_0(\eta) + f_1(\eta) + \cdots, \tag{15a}$$

$$\theta = X^{-1/3} g_0(\eta) + X^{-2/3} g_1(\eta) + \cdots , \tag{15b}$$

where the similarity variables is

$$\eta = Y / X^{2/3}. \tag{16}$$

The plume now has centreline at $Y = 0$, and the plume ascends along the X-axis. The equations for f_0, g_0, f_1 and g_1 are

$$C f_0'' - D g_0' = 0, \tag{17a}$$

$$g_0'' + \frac{1}{3}(f_0 g_0)' = 0, \tag{17b}$$

$$C f_1'' - D g_1' = \frac{2}{3} B (f_0' + 2\eta f_0'') - \frac{1}{3} D \tan\delta (g_0 + 2\eta g_0'), \tag{17c}$$

$$g_1'' + \frac{1}{3} f_0 g_1' + \frac{2}{3} f_0' g_1 + \frac{1}{3} f_1' g_0 = 0, \tag{17d}$$

and the heat flux constraints become,

$$\int_{-\infty}^{\infty} f_0' g_0 \, d\eta = 1, \tag{18a}$$

$$\int_{-\infty}^{\infty} \left[f_0' g_1 + f_1' g_0 + \left[\frac{1}{3}(f_0 - 2\eta f_0') g_0 + g_0' \right] \tan\delta \right] d\eta = 0, \tag{18b}$$

where we note that the term multiplying $\tan\delta$ integrates to zero because of the symmetry of the integrand. The boundary conditions for the leading order terms are

$$f_0(0) = g_0'(0) = 0 \quad \text{and} \quad f_0', g_0 \to 0 \quad \text{as} \quad \eta \to \pm\infty, \tag{19a}$$

and, for the first order terms,

$$g_1 \to 0 \quad \text{as} \quad \eta \to \pm\infty. \tag{19b}$$

The other conditions necessary to solve Equations (17c,d) must be determined by asymptotic matching with the solutions from the outer regions since it is the latter which induces the corrections represented by f_1 and g_1.

As noted by Afzal (1985) and Bassom *et al.* (2001) there exist exact closed-form solutions of the leading and first order equations, (17a)–(17d), which satisfy the heat flux relations (18a) and (18b). Using the scaled independent variable

$$\zeta = \frac{1}{6} a_0 \eta, \tag{20}$$

the new coefficient functions, F_0, G_0, F_1 and G_1 are defined by

$$f_0(\eta) = a_0 F_0(\zeta), \qquad g_0(\eta) = b_0 G_0(\zeta), \tag{21a}$$

$$f_1(\eta) = a_1 F_1(\zeta), \qquad g_1(\eta) = b_1 G_1(\zeta), \tag{21b}$$

where

$$a_0 = \left(\frac{9D}{2C}\right)^{1/3}, \qquad b_0 = \left(\frac{3C}{32D}\right)^{1/3}, \tag{22a}$$

$$a_1 = \frac{4}{C}, \qquad b_1 = \frac{2a_0}{3D}. \tag{22b}$$

On substituting expressions (20), (21) and (22) into Equations (17a)–(17d) and (18a) and (18b), we obtain the following equations,

$$F_0'' - G_0' = 0, \qquad G_0'' + 2(F_0 G_0)' = 0, \tag{23a, b}$$

$$F_1'' - G_1' = \hat{B}(F_0' + \zeta F_0''), \qquad G_1'' + 2F_0 G_1' + 4F_0' G_1 + 2F_1' G_0 = 0, \tag{23c, d}$$

where

$$\hat{B} = B - \frac{3b_0 D \tan\delta}{a_0^2}, \tag{23e}$$

and the constraints,

$$\int_{-\infty}^{\infty} F_0' G_0 \, d\zeta = \frac{4}{3}, \qquad \int_{-\infty}^{\infty} (F_0' G_1 + F_1' G_0) d\zeta = 0. \tag{24a, b}$$

The closed-form solutions are

$$F_0 = \tanh\zeta, \qquad G_0 = \operatorname{sech}^2\zeta, \tag{25a, b}$$

$$F_1 = \hat{B}\,[\zeta F_0 - 2\ln(\cosh\zeta)] + M_1 + M_2 F_0' + M_3(\zeta F_0' + F_0 - 2\zeta), \tag{26a}$$

$$G_1 = \hat{B}(-\zeta F_0') + M_2 F_0'' + M_3(\zeta F_0'' + 2F_0'), \tag{26b}$$

where we have imposed exponential decay on the temperature as $\zeta \to \pm\infty$. Furthermore, M_1, M_2 and M_3 are constants of integration. For an isotropic medium with $\delta = 0$, that is $C = D = 1$, the leading order solution reduces to that given by Wooding (1963) and Afzal (1985).

Note that $F_1 \sim -(\pm\hat{B} + 2M_3)\zeta$ as $\zeta \to \pm\infty$, which provides matching conditions for the outer region solutions. As $\hat{B}$ is dependent on the unknown direction of the plume, δ, via (23e), the satisfaction of the matching conditions will yield this

angle. But matching with the outer regions requires the use of polar coordinates, r and Φ, where $\Phi = \phi - \delta$ is the angular coordinate relative to the plume centreline. On using $\eta = r^{1/3} \sin\Phi/(\cos\Phi)^{2/3}$ we expand for small values of Φ to obtain the behaviour of ψ as $\eta \to \pm\infty$:

$$\psi \sim r^{1/3}\left[a_0 - \frac{1}{6}a_0 a_1(\hat{B} + 2M_3)\Phi\right] \quad \text{as} \quad \eta \to \infty, \tag{27a}$$

and

$$\psi \sim r^{1/3}\left[-a_0 + \frac{1}{6}a_0 a_1(\hat{B} - 2M_3)\Phi\right] \quad \text{as} \quad \eta \to -\infty. \tag{27b}$$

The first terms in (27a) and (27b) are equivalent to the inflow to the plume which induces the leading order flow in the outer regions. The second terms reflect how the outer flow, in its turn, alters the behaviour of the plume.

3.2. THE OUTER REGIONS

As the thermal field decays exponentially out of the boundary layer we may neglect thermal effects. The governing equation becomes

$$\bar{A}\frac{\partial^2\psi}{\partial r^2} + \frac{2}{r}\bar{B}\left(\frac{\partial^2\psi}{\partial r\partial\Phi} - \frac{1}{r}\frac{\partial\psi}{\partial\Phi}\right) + \frac{1}{r}\bar{C}\left(\frac{1}{r}\frac{\partial^2\psi}{\partial\Phi^2} + \frac{\partial\psi}{\partial r}\right) = 0, \tag{28}$$

and

$$\bar{A} = A\cos^2\Phi + B\sin 2\Phi + C\sin^2\Phi, \tag{29a}$$

$$\bar{B} = \frac{1}{2}(C - A)\sin 2\Phi + B\cos 2\Phi, \tag{29b}$$

$$\bar{C} = A\sin^2\Phi - B\sin 2\Phi + C\cos^2\Phi. \tag{29c}$$

In view of the leading behaviour of ψ as given in (27) the outer region expansion begins as

$$\psi = r^{1/3}\mathcal{F}(\Phi) + \cdots, \tag{30}$$

where $\mathcal{F}$ satisfies,

$$\bar{C}\mathcal{F}'' - \frac{4}{3}\bar{B}\mathcal{F}' + \frac{1}{3}\left(\bar{C} - \frac{2}{3}\bar{A}\right)\mathcal{F} = 0. \tag{31}$$

The boundary conditions which are satisfied by $\mathcal{F}$ depend on the flow configuration.

When there are no bounding surfaces there is only one outer region and we solve Equation (31) subject to the four boundary conditions which are taken from the asymptotic relation (27):

$$\mathcal{F}(0) = a_0, \qquad \mathcal{F}'(0) = -\frac{1}{6}a_0 a_1(\hat{B} + 2M_3), \tag{32a}$$

$$\mathcal{F}(2\pi) = -a_0, \qquad \mathcal{F}'(2\pi) = \frac{1}{6}a_0 a_1(\hat{B} - 2M_3). \tag{32b}$$

Although (31) forms a second order system, the third and fourth equations may be taken to be

$$\delta' = 0, \qquad M_3' = 0, \tag{33}$$

since both δ and M_3 are constants, and we may therefore apply a straightforward boundary value problem solver to the complete 4th order system.

When there are two bounding surfaces there exist two outer regions. If we denote the solution in the outer region occupying $\Phi > 0$ by $\mathcal{F}_+$ and the other by $\mathcal{F}_-$, then we need to solve the 6th order system,

$$\bar{C}\mathcal{F}_+'' - \frac{4}{3}\bar{B}\mathcal{F}_+' + \frac{1}{3}(\bar{C} - \frac{2}{3}\bar{A})\mathcal{F}_+ = 0, \tag{34a}$$

$$\bar{C}\mathcal{F}_-'' - \frac{4}{3}\bar{B}\mathcal{F}_-' + \frac{1}{3}(\bar{C} - \frac{2}{3}\bar{A})\mathcal{F}_- = 0, \tag{34b}$$

$$\delta' = 0, \qquad M_3' = 0, \tag{34c}$$

subject to the boundary conditions,

$$\mathcal{F}_+(0) = a_0, \qquad \mathcal{F}_+'(0) = -\frac{1}{6}a_0 a_1(\hat{B} + 2M_3), \tag{35a}$$

$$\mathcal{F}_-(0) = -a_0, \qquad \mathcal{F}_-'(0) = \frac{1}{6}a_0 a_1(\hat{B} - 2M_3), \tag{35b}$$

$$\mathcal{F}_+(\phi^+ - \delta) = 0, \qquad \mathcal{F}_-(\phi^- - \delta) = 0. \tag{35c}$$

Since δ is unknown, the ranges of integration for both $\mathcal{F}_+$ and $\mathcal{F}_-$ are also unknown. However, it is very straightforward to alter the range of integration for both functions to the interval 0 to 1 by a linear coordinate transformation. In this way all the unknown values and functions form part of either the equations or the boundary conditions.

4. Results and Discussion

Our numerical results were obtained using a 4th order Runge–Kutta scheme allied to the shooting method. In all cases we used 200 intervals which yields solutions

which are correct to more than four significant figures. In all the different types of configuration we consider, none of the initial conditions are known (for example, the value a_0 which is used in (32) and (35) is a function of δ) and therefore it proves necessary to iterate for all initial conditions.

The full parameter set comprises the three rotation angles for the principal axes, two permeability ratios, and either zero, one or two angles of the bounding surfaces. Clearly it is impossible to present a comprehensive account of the effect of varying each parameter, and for this reason we have decided to confine our interest to those configurations for which the principal axes have been rotated about the z-axis, and therefore we take $\alpha = \beta = 0$. This means that the principal axes corresponding to K_1 and K_2 make an angle γ to the vertical and horizontal, respectively. We consider three special cases:

Case 1. An isolated line heat source (no bounding surfaces).

Case 2. A single bounding surface located at $\phi = \gamma + 180°$.

Case 3. Two bounding surfaces located at $\phi = \gamma \pm 90°$.

Case 2 corresponds to where the two bounding surfaces are effectively coincident and hence $\phi^+ - \phi^- = 360°$. Case 3 has the line source embedded in a plane and this corresponds to $\phi^+ - \phi^- = 180°$. For all these cases there are two parameters, γ, the rotation angle of the principal axes about the z-axis, and $\xi = K_1/K_2$, the permeability ratio. For Case 2 the single bounding surface lies in the direction opposing the principal axis corresponding to K_1. Here we take $\phi^+ = \gamma + 180°$ and $\phi^- = \gamma - 180°$. For Case 3 the two bounding surfaces are parallel to the K_2 principal axis.

Our restricted sets of results are shown in Figures 2, 3 and 4 which correspond respectively to Cases 1, 2 and 3. Indications of the directions of the principal axes and their relation to the direction of the bounding surfaces are depicted schematically below each Figure. All angles are expressed in terms of degrees, for convenience.

Figure 2 shows how the orientation of the plume varies with γ for various permeability ratios ξ. Values of ξ which are greater than 1 correspond to cases where $K_2 < K_1$. When $\xi > 1$ the plume takes positive orientations as γ increases from zero. The reason for this is that flow in the direction given by the K_1 axis is favoured. For relatively high values of ξ the plume travels very easily in that direction and this yields the large positive values of δ. For example, for $\xi = 100$, which is an example of a rather extremely anisotropic medium, the plume orientation curve is close to the line $\delta = \gamma$ which indicates that the plume centreline is in the positive K_1 direction. When ξ takes more realistic values much closer to 1 the variation in the plume orientation is more sedate and the maximum orientation of the plume remains close to the vertical. This may be seen in Table I where we indicate how the maximum absolute deviation of the plume centreline from the vertical varies with ξ. When ξ is close to 1 (so that the medium is nearly isotropic) the maximum plume deflection takes place when the rotation of the principal axes is close to 45°. Finally we note that certain symmetries are present in these Case 1

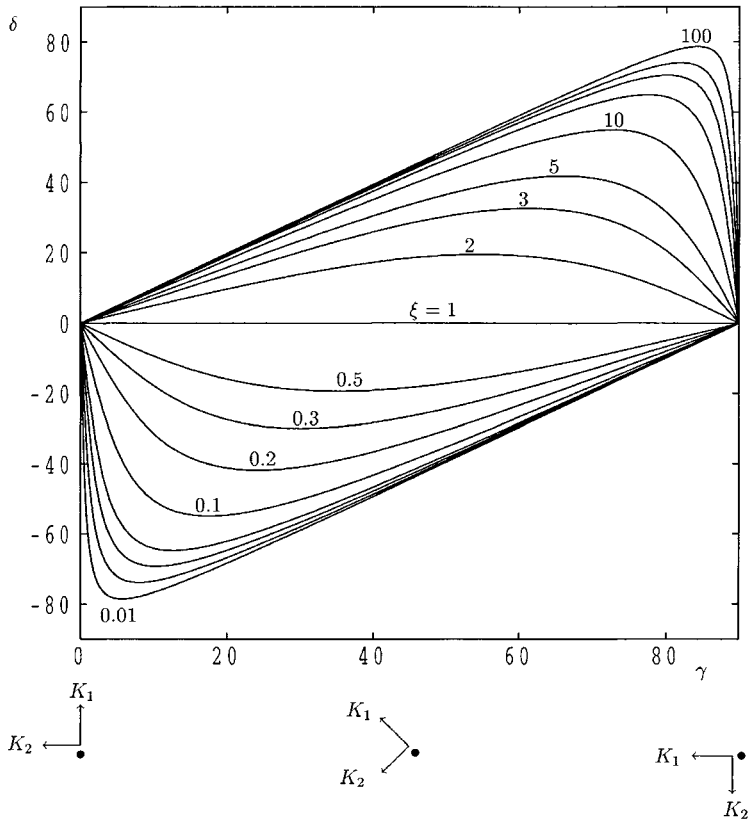

Figure 2. The variation of the plume deflection angle, δ, with the principal axis rotation angle, γ, for various values of the permeability ratio, ξ, for plume convection from an isolated line heat source. The values of ξ represented are 0.01, 0.02, 0.03, 0.05, 0.1, 0.2, 0.3, 0.5, 1, 2, 3, 5, 10, 20, 30, 50, 100. Also shown is a schematic of the relation between the principal axes and γ.

results and therefore we have restricted the values of γ presented in Figure 2 for the range $0 \leqslant \gamma \leqslant 90°$. Plume deflections at other angles may be found using the relation

$$\delta(\gamma, \xi) = \delta(\gamma + 90°, \xi^{-1}). \tag{36}$$

Figure 3 represents the case of one isolated semi-infinite surface with leading edge at the line source. When $\gamma = 0$ the surface is vertical and lies directly below the line source.

For small values of γ the overall effect of the presence of the surface is small compared with the isolated source shown in Figure 2, and similar physical arguments apply. However, the difference between Cases 1 and 2 becomes very significant when γ gets close to 90° especially for those media where $\xi > 1$. Again taking the $\xi = 100$ curve as an extreme example, we have a large positive plume

Table I. Values of γ which maximise the plume inflection for the given values of ξ

ξ	δ	γ
0.999	−0.2866	44.9857
0.99	−0.2879	44.856
0.9	−3.017	43.492
0.8	−6.379	41.810
0.5	−19.471	35.264
0.3	−32.579	28.711
0.2	−41.810	24.095
0.1	−54.903	17.548
0.05	−64.791	12.604
0.03	−70.347	9.826
0.02	−73.901	8.049
0.01	−78.579	5.711
0.001	−86.378	1.811

Also shown are the corresponding plume deflections, δ. Corresponding values for $\xi > 1$ may be obtained using $\delta(\xi^{-1}) = -\delta(\xi)$ and $\gamma(\xi^{-1}) = 90 - \gamma\ (\xi)$.

deflection when γ is just less than 90°. At this point the fluid prefers to travel in the positive K_1 direction which lies just above the horizontal. However, as the inclination of the surface and the principal axes increases to values just greater than 90°, buoyancy forces still require fluid to rise, but the easiest path is now in the negative K_1 direction, which explains the large negative values of δ. There is a relatively quick transition between the large positive and large negative deflections as γ passes through 90°. Again, less severe plume deviations arise for more realistic values of ξ.

In Figure 3 we confine the presentation of the dependence of δ on γ to the range $0° \leqslant \gamma \leqslant 180°$. At $\gamma = 180°$ the isolated surface is vertical and the plume deviation is positive in all cases considered. At such values of γ we feel it is very likely that the plume will attach itself to the surface in the same way that free jets are attracted towards adjacent surfaces due to the lack of fluid to entrain. This is almost certainly the case for an isotropic medium given by $\xi = 1$ for then a straightforward vertical plume will arise in practice, even though the present analysis predicts a deviation of approximately 55°. For $\xi = 1$ it is also possible to obtain $\delta \simeq -55°$ when $\gamma = -180°$ which is essentially the same case as for $\gamma = 180°$, and hence there are three possible solutions for the isolated vertical surface laying immediately above the line source. Although these nonvertical mathematical solutions are valid solutions of the equations, we believe that they are likely to be unstable, and the definitive demonstration of this conjecture will lie in the computation of the stability characteristics of plumes using an unsteady elliptic

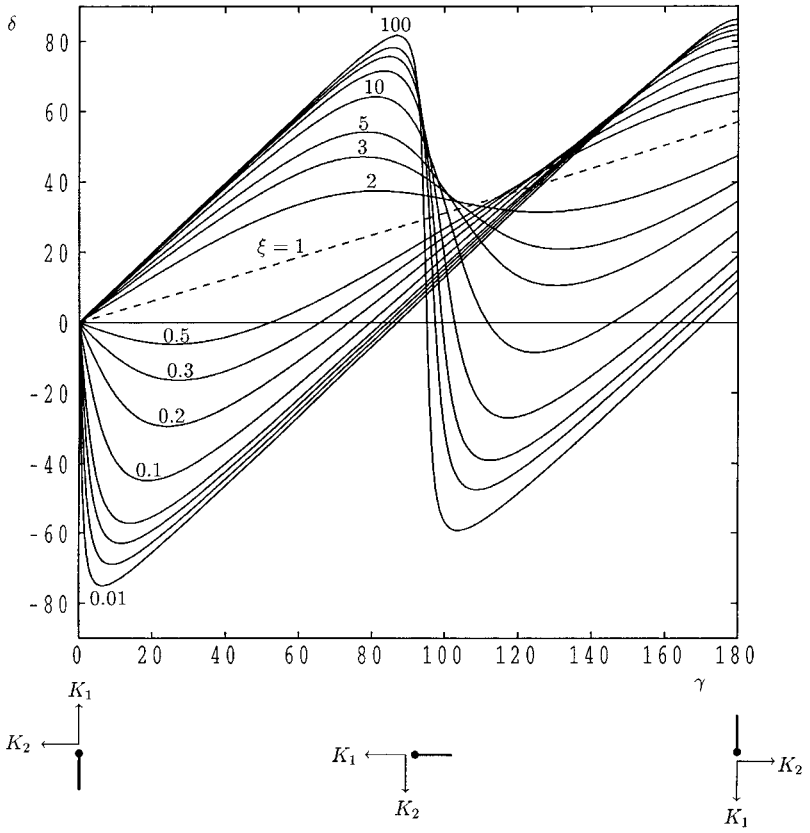

Figure 3. The variation of the plume deflection angle, δ, with the principal axis rotation angle, γ, for various values of the permeability ratio, ξ, for plume convection from a line heat source in the presence of an isolated semi-infinite surface located at $\phi = \gamma + 180°$. The values of ξ represented are 0.01, 0.02, 0.03, 0.05, 0.1, 0.2, 0.3, 0.5, 1, 2, 3, 5, 10, 20, 30, 50, 100. Also shown is a schematic of the relation between the principal axes and γ.

formulation of the governing equations. However, we point out that the solutions presented here assume from the outset that the flow has a certain structure, namely that the plume boundary layer is bordered by two different outer flow regions. Thus the flow represented by Figure 3 are possible solutions of the governing equations, but when γ get close to 180°, they may not represent stable solutions.

In Figure 4 we display how δ varies with γ for a semi-infinite porous medium. Here we restrict attention to cases for which $0 \leqslant \gamma \leqslant 90°$. When $\gamma > 90°$ one of the bounding surfaces lies above the plume and while the numerical solutions represent valid solutions of the equations, they are highly likely to be unstable. Here the variation of δ with γ follows the same trends as in Figures 2 and 3 when γ is small. When γ reaches values close to 90° we again have positive value of δ for all anisotropies depicted, although the plume deviation when the medium is isotropic is now approximately 50° due to the slightly different outer flow field.

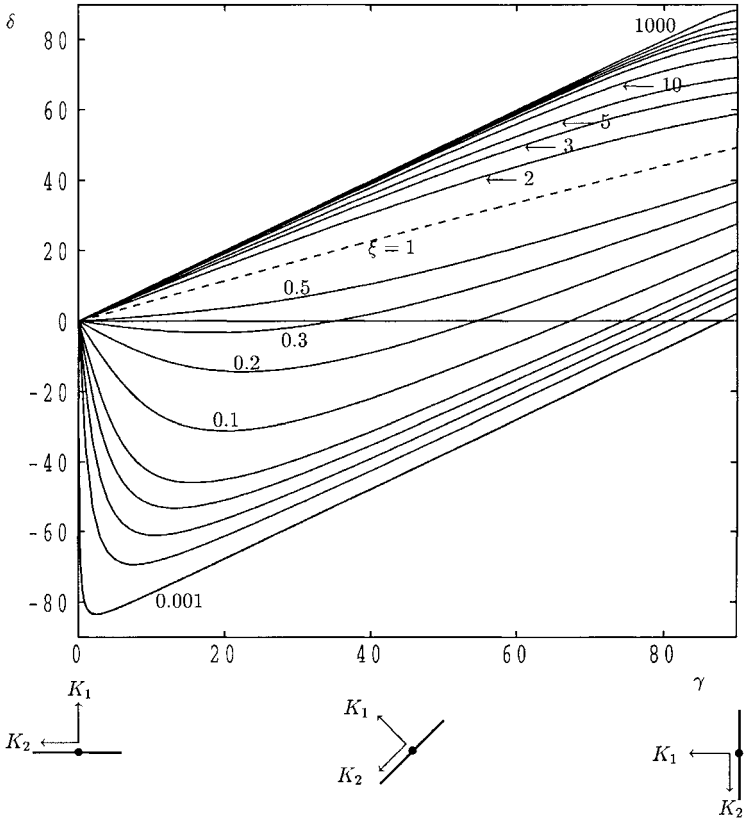

Figure 4. The variation of the plume deflection angle, δ, with the principal axis rotation angle, γ, for various values of the permeability ratio, ξ, for plume convection from a line heat source embedded in a plane with normal in the same direction as the K_1 principal axis. The values of ξ represented are 0.001, 0.01, 0.02, 0.03, 0.05, 0.1, 0.2, 0.3, 0.5, 1, 2, 3, 5, 10, 20, 30, 50, 100 and 1000. Also shown is a schematic of the relation between the principal axes and γ.

We note that, for $\xi > 0.428$ the plume always has a positive deviation; for other values of ξ deviations may be either positive or negative depending on the value of γ.

5. Conclusions

We find that the presence of anisotropy causes plumes to rise at angles other than the vertical in general. In this regard anisotropy has a similar effect to the presence of asymmetrically placed (relative to the vertical) bounding surfaces in an isotropic porous medium; see Bassom *et al.* (2001). This feature, which is well known in the analysis of contaminant movement in groundwater studies, is somewhat unexpected in the free convective context where there is no imposed pressure gradient causing mixed convective transport.

From a mathematical point of view the lesson to be gleaned from the present paper is that it is not always sufficient simply to consider the leading order boundary layer flow when analysing plumes. A naive analysis which does not consider the outer flow regions and their effect on the next correction to the plume solution, is likely to assume that the plume rises vertically, and hence the results of such an analysis will be incorrect. Even if one assumes that it rises at a different angle, there is no rational argument for an a priori choice of an angle unless the analysis presented here is followed. Indeed we have shown that it is absolutely essential to allow the plume to deviate by an O(1) angle from the vertical in order to be able to obtain a solution for the second term in the asymptotic expansion. We note that such a mathematical device, whereby O(1) effects are determined by the solution of equations at higher order, is quite commonplace in the context of the theory of weakly nonlinear Bénard convection (see Newell and Whitehead, 1969, for example) and other weakly nonlinear and WKBJ theories.

We have seen that the plume is strongly attracted to the direction of that principal axis corresponding to the larger permeability, especially when permeability ratio is substantially different from 1. But when $\gamma \neq 0$ the flows are never in those precise directions because of twin effects of buoyancy, which serves to cause the fluid to rise vertically, and the presence of external boundaries, which modifies the detailed flow outside the plume and which, in turn, affects the position of the plume quite strongly.

Appendix

In this Appendix we present the definitions of the entries of the diffusivity tensor given in Equation (3).

$$\begin{aligned} K_1 L_{11} &= K_1 \cos^2\beta \cos^2\gamma + \\ &\quad + K_2(\sin\alpha \sin\beta \cos\gamma - \cos\alpha \sin\gamma)^2 + \\ &\quad + K_3(\cos\alpha \sin\beta \cos\gamma + \sin\alpha \sin\gamma)^2, \end{aligned} \tag{A1}$$

$$\begin{aligned} K_1 L_{22} &= K_1 \cos^2\beta \sin^2\gamma + \\ &\quad + K_2(\sin\alpha \sin\beta \sin\gamma + \cos\alpha \cos\gamma)^2 + \\ &\quad + K_3(\cos\alpha \sin\beta \sin\gamma - \sin\alpha \cos\gamma)^2, \end{aligned} \tag{A2}$$

$$K_1 L_{33} = K_1 \sin^2\beta + K_2 \sin^2\alpha \cos^2\beta + K_3 \cos^2\alpha \cos^2\beta, \tag{A3}$$

$$\begin{aligned} K_1 L_{12} = K_1 L_{21} &= K_1 \cos^2\beta \sin\gamma \cos\gamma + K_2(\sin\alpha \sin\beta \cos\gamma - \\ &\quad - \cos\alpha \sin\gamma)(\sin\alpha \sin\beta \sin\gamma + \cos\alpha \cos\gamma) + \\ &\quad + K_3(\cos\alpha \sin\beta \cos\gamma + \sin\alpha \sin\gamma) \times \\ &\quad \times (\cos\alpha \sin\beta \sin\gamma - \sin\alpha \cos\gamma), \end{aligned} \tag{A4}$$

$$K_1L_{13} = K_1L_{31} = -K_1 \sin\beta \cos\beta \cos\gamma + \\ + K_2(\sin\alpha \sin\beta \cos\gamma - \cos\alpha \sin\gamma) \sin\alpha \cos\beta + \\ + K_3(\cos\alpha \sin\beta \cos\gamma + \sin\alpha \sin\gamma) \cos\alpha \cos\beta, \quad \text{(A5)}$$

$$K_1L_{23} = K_1L_{32} = K_1 \sin\beta \cos\beta \sin\gamma + \\ + K_2(\sin\alpha \sin\beta \sin\gamma + \cos\alpha \cos\gamma) \sin\alpha \cos\beta + \\ + K_3(\cos\alpha \sin\beta \sin\gamma - \sin\alpha \cos\gamma) \cos\alpha \cos\beta. \quad \text{(A6)}$$

The expressions (A1)–(A6) correspond to expressions (A1)–(A6) given in Rees and Storesletten (1995), but in that paper there were several misprints concerning the signs in (A1), (A2), (A4), (A5) and (A6).

6. Acknowledgement

L. Storesletten gratefully acknowledges financial support from the Norwegian Research Council during his sabbatical leave at the University of Bath, Autumn 2000.

References

Afzal, N.: 1985, Two-dimensional buoyant plume in porous media: higher-order effects, *Int. J. Heat Mass Transfer* **28**, 2029–2041.

Bassom, A. P., Rees, D. A. S. and Storesletten, L.: 2001, Convective plumes in porous media: the effect of asymmetrically placed boundaries, *Int. Comm. Heat Mass Transfer* **28**(1), 31–38.

Ene, H. I.: 1991, Effect of anisotropy on the free convection from a vertical plate embedded in a porous medium, *Transport in Porous Media* **6**, 183–194.

Gebhart, B.: 1979, Buoyancy induced fluid motions characteristic of applications in technology, *Trans. A.S.M.E. J. Fluids Eng.* **101**, 5–28.

Harter, T. and Yeh, T.-C. J.: 1996a, Stochastic analysis of solute transport in heterogeneous, variably saturated soils, *Water Resour. Res.* **32**, 1585–1595.

Harter, T. and Yeh, T.-C.J.: 1996b, Conditional stochastic analysis of solute transport in heterogeneous, variably saturated soils, *Water Resour. Res*. **32**, 1597–1609.

Newell, A. C. and Whitehead, J. A.: 1969, Finite bandwidth, finite amplitude convection, *J. Fluid Mech.* **38**, 279–303.

Rees, D. A. S. and Storesletten, L.: 1995, The effect of anisotropic permeability on free convective boundary layer flow in porous media, *Transport in Porous Media* **19**, 79–92.

Shaw, D.C.: 1985, The asymptotic behaviour of a curved line source plume within an enclosure, *I.M.A. J Appl. Math.* **35**, 71–89.

Storesletten, L. and Rees, D. A. S.: 1997, An analytical study of free convective boundary layer flow in porous media: the effect of anisotropic diffusivity, *Transport in Porous Media* **27**, 289–304.

Wooding, R. W.: 1963, Convection in a saturated porous medium at large Rayleigh number or Peclet number, *J. Fluid Mech.* **15**, 527–544.